Proceedings of
2003 ASME Summer Heat Transfer Conference
July 21-23, 2003, Las Vegas, Nevada, USA

ASME2003-47109

A SIMPLE HEAT TRANSFER CORRELATION FOR THREE INLET CONFIGURATIONS USING ARTIFICIAL NEURAL NETWORK IN THE COMPLEX TRANSITION FLOW REGIME

A. J. Ghajar, School of Mechanical and Aerospace Engineering, Oklahoma State University, Stillwater, Oklahoma, 74048, USA. Phone:(405) 744-5900, Fax:(405) 744-7873, email: ghajar@okstate.edu

S. C. Tam, Department of Mathematics, Faculty of Science and Technology, University of Macau. P.O. Box 3001, Taipa, Macau, China

L. M. Tam, Department of Electromechanical Engineering, Faculty of Science and Technology, University of Macau, Macau. P.O. Box 3001, Taipa, Macau, China

ABSTRACT

Local forced and mixed heat transfer coefficients were measured by Ghajar and Tam (1994) along a stainless steel horizontal circular tube fitted with reentrant, square-edged, and bell-mouth inlets under uniform wall heat flux condition. For the experiments the Reynolds, Prandtl, and Grashof numbers varied from about 280 to 49000, 4 to 158, and 1000 to 2.5×10^5, respectively. The heat transfer transition regions were established by observing the change in the heat transfer behavior. The data in the transition region were correlated by using the traditional least squares method. The correlation predicted the transitional data with an average absolute deviation of about 8%. However, 30% of the data were predicted with 10 to 20% deviation. The reason is due to the abrupt change in the heat transfer characteristic and its intermittent behavior. Since the value of heat transfer coefficient has a direct impact on the size of the heat exchanger, a more accurate correlation has been developed using the artificial neural network (ANN). A total of 1290 data points (441 for reentrant, 416 for square-edged, and 433 for bell mouth) were used. The accuracy of the new correlation is excellent with the majority of the data points predicted with less than 10% deviation.

INTRODUCTION

An important design problem in industrial heat exchangers arises when flow inside the tubes falls into the transition region. In practical engineering design, the usual recommendation is to avoid design and operation in this regime; however, this is not always feasible under design constraints. The usually cited transition Reynolds number of about 2100 applies, strictly speaking, to a very steady and uniform entry flow with a rounded entrance. If the flow has a disturbed entrance typical of heat exchangers, in which there is a sudden contraction and possibly even a reentrant entrance, the transition Reynolds number will be less. Experimental, numerical, and analytical studies are available for forced and mixed convection heat transfer in horizontal tubes with a rounded entrance in the laminar, transitional, and turbulent flow regimes. These works have been reviewed by Shah and London (1978), Shah and Johnson (1981), and Kakac and coworkers (1981 and 1987). However, very little information that is of immediate use to design engineers (i.e., correlation) is available to predict the developing and fully developed transitional forced and mixed convection heat transfer coefficients in a tube with a smooth or disturbed entrance. The correlation developed by Ghajar and Tam (1994) is the only one that is available in the open literature for the above-mentioned case. Their correlation predicted the transitional data with an average absolute deviation of about 8%. However, 30% of the data were

Copyright © 2003 by ASME

predicted with 10 to 20% deviation. Since the value of heat transfer coefficient has a direct impact on the size of the heat exchanger, an accurate correlation is necessary. Because the traditional least-squares method did not provide the desired accuracy for all the data points, an alternative method, the artificial neural network (ANN) is employed. ANN has been successfully used in the analysis of heat transfer data and evaluation of heat transfer coefficient by Thibault and Grandjean (1991) and Jambunathan et al. (1996). The applications of ANN in different areas in thermal engineering are well described in the comprehensive work done by Sen and Yang (1999). Diaz et al. (1999), Pacheco-Vega et al. (2001a), Diaz et al. (2001) and Pacheco-Vega et al. (2001b). In the work done in Pecheco-Vega et al. (2001), ANN and least squares methods were used to correlate the heat transfer coefficient and the heat transfer rate directly. The results show that direct correlation for heat transfer rate is more accurate than the heat transfer coefficient. Direct prediction of heat transfer rate can help user in evaluating the performance of heat exchanger easily, however, if the design of heat exchanger is the objective, the fundamental, which is the determination of heat transfer coefficient, i.e., the Nusselt number, is still absolutely necessary. The purpose of this study was to create an accurate correlation using an unconventional method to correlate experimental data for a wide range of Reynolds, Prandtl, and Grashof numbers in the entrance and fully developed regions of a circular horizontal electrically heated straight tube fitted with three different inlet configurations (reentrant, square-edged, and bell-mouth).

NOMENCLATURE

a = layer output vector
b = bias
c_p= specific heat of the test fluid at the bulk temperature
D = inside diameter of tube
f = activation function
Gr = local bulk Grashof number, $g\beta\rho^2D^3(T_w - T_b)/\mu^2$
h = local average or fully developed peripheral heat transfer coefficient
k = thermal conductivity of the test fluid at the bulk temperature
n = net input column vector
Nu = local Nusselt number, hD/k
Pr = local bulk Prandtl number, $\mu c_p /k$
Re = local bulk Reynolds number, $\rho V D/ \mu$
T = temperature
u = constant matrix
v = constant matrix
V = average velocity in the test section
W = weight matrix
x = local distance
ρ = density of the test fluid at the bulk temperature
μ = dynamic viscosity

Superscript
m = layer

Subscripts
b = bulk
l = laminar
R = number of network input
S = number of neurons
t = turbulent
tr = transition
w = wall

HEAT TRANSFER EXPERIMENTS

The heat transfer experimental data used in this study along with a detailed description of the experimental apparatus and procedures used were reported by Ghajar and Tam (1994). A schematic of the overall experimental setup used for heat transfer measurements is shown as Fig.1. In this paper only a brief description of the experimental setup and procedures will be provided. The local forced and mixed convective measurements were made in a horizontal electrically heated stainless steel circular straight tube with reentrant, square edged, and bell-mouth inlets under uniform wall heat flux condition. The pipe had an inside diameter of 1.58 cm and an outside diameter of 1.90 cm. The total length of the test section was 6.10 m, providing a maximum length-to-diameter ratio of 385. A uniform wall heat flux boundary condition was maintained by a dc arc welder. Thermocouples (T-type) were placed on the outer surface of the tube wall at close intervals near the entrance and at greater intervals further downstream. Twenty-six axial locations were designated, with four thermocouples placed at each location. The thermocouples were placed 90^o apart around the periphery. From the local peripheral wall temperature measurements at each axial location, the inside wall temperatures and the local heat transfer coefficients were calculated. In these calculations, the axial conduction was assumed negligible (RePr > 4,200 in all cases), but peripheral and radial conduction of heat in the tube wall were included. In addition, the bulk fluid temperature was assumed to increase linearly from the inlet to the outlet. As reported by Ghajar and Tam (1994), the uncertainty analyses of the overall experimental procedures showed that there is a maximum of 9% uncertainty for the heat transfer coefficient calculations. Moreover, the heat balance error for each experimental run indicates that in general, the heat balance error is less than 5%. For Reynolds numbers lower than 2500 where the flow is strongly influenced by secondary flow, the heat balance error is

Copyright © 2003 by ASME

relatively higher (5 to 8%) for that particular Reynolds number range.

To ensure a uniform velocity distribution in the test fluid before it entered the test section, the flow passed through calming and inlet sections. The calming section had a total length of 61.6 cm and consisted of a 17.8-cm-diameter acrylic cylinder with three perforated acrylic plates followed by tightly packed soda straws sandwiched between galvanized steel mesh screens. Before entering the inlet section, the test fluid passed through a fine mesh screen and flowed undisturbed through 23.5 cm of a 6.5-cm-diameter acrylic tube before it entered the test section. The inlet section had the versatility of being modified to incorporate a reentrant or bell mouth inlet (see Fig. 2). The reentrant inlet was simulated by sliding 1.91 cm of the tube entrance length into the inlet section, which was otherwise the square-edged (sudden contraction) inlet. For the bell-mouth inlet, a fiberglass nozzle with contraction ratio of 10.7 and a total length of 23.6 cm was used in place of the inlet section.

In the experiments, distilled water and mixtures of distilled water and ethylene glycol were used. The experiments covered the local bulk Reynolds number range 280 to 49000, the local Prandtl number range 4 to 158, the local bulk Grashof number range 1000 to 2.5×10^5, and the local bulk Nusselt number range 13 to 258. The wall heat flux for the experiments ranged from 4 to 670 kW/m^2.

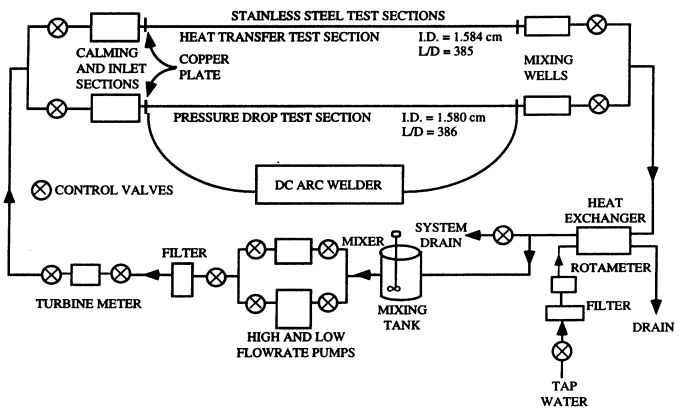

Figure 1 Schematic diagram of experimental setup

CORRELATION USING ARTIFICIAL NEURAL NETWORK

Figure 3 shows the heat transfer data for the transition region for the reentrant, square-edged, and bell-mouth inlet configurations. The figure clearly shows the influence of inlet configuration on the beginning and end of the heat transfer transition region. Figure 3 plots the local average peripheral heat transfer coefficients in terms of the Colburn j factor ($StPr^{0.6}$) versus local bulk Reynolds number for all flow regimes at the length-to-diameter ratio of 192. The filled symbols represent the start and end of the heat transfer transition region for each inlet configuration.

Figure 3, for comparison purposes, also shows the typical fully developed pipe flow forced convection heat transfer correlations for turbulent (Sieder and Tate, 1936) and laminar (Nu=4.364) flows under the uniform wall heat flux boundary condition. In the turbulent flow regime, for Reynolds numbers greater than about 8500 to 10,500 (depending on the inlet type), the experimental data appear on the turbulent heat transfer line (within ± 8%). However, in the laminar flow regime, for Reynolds numbers less than about 2000 to 3800 (depending on the inlet type), the data appear to have a pronounced and almost parallel shift above the accepted laminar heat transfer line. This is directly due to the strong influence of buoyancy forces (free convection) on forced convection, giving rise to mixed convection heat transfer. This in turn results in a higher fully developed laminar uniform wall heat flux Nusselt number than the accepted 4.364 value (a value about 14.5 is estimated for the data). It should be noted that in the fully developed laminar flow region no forced convection data could be obtained. At the minimum welder current setting (approximately 150 A), the heat generated at the tube wall was enough to bring about peripheral temperature variations extensive enough to cause secondary flow.

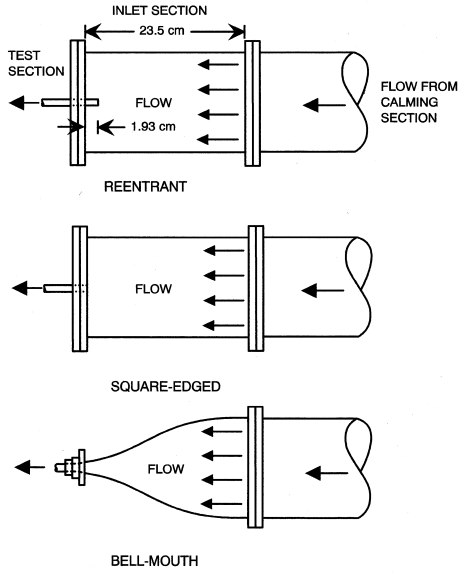

Figure 2 Schematic of the three different inlet configurations

As seen in Fig. 3, the abrupt change of heat transfer characteristic in the transition region is obvious. In this region the flow has both laminar and turbulent characteristics. In addition, the type of inlet configuration influences the beginning and end of the transition region. Ghajar and Tam (1994) used

Copyright © 2003 by ASME

the asymptotic method similar to Churchill (1977) to develop a correlation in the transition region since the variation of heat transfer coefficient, as indicated by Fig. 3 is between two asymptotes. The correlation is

$$Nu_{tr} = Nu_l + \{\exp[(a\text{-}Re)/b] + Nu_t^c\}^c \quad (1)$$

where Nu_l (laminar flow Nusselt number) is given by Eq. (2), Nu_t (turbulent flow Nusselt number) is given by Eq. (3), and the values of the suggested constants a, b, and c for each inlet are summarized in Table 1.

$$Nu_l = 0.61[(RePrD/x)+0.025(GrPr)^{0.8}]^{0.4}(\mu_b/\mu_w)^{0.14} \quad (2)$$

$$Nu_t = 0.023Re^{0.8}\, Pr^{0.385}(x/D)^{-0.0054}(\mu_b/\mu_w)^{0.14} \quad (3)$$

Table 1. Constants for Eq. (1)

Inlet	a	b	c
Reentrant	1766	276	-0.955
Square-edged	2617	207	-0.950
Bell-mouth	6628	237	-0.980

The range of independent variables used in Eq. (1) is as follows:

Reentrant

$3 \le x/D \le 192$, $1700 \le Re \le 9100$, $5 \le Pr \le 51$,
$4000 \le Gr \le 2.1\times10^5$, and $1.2 \le \mu_b/\mu_w \le 2.2$

Square-edged

$3 \le x/D \le 192$, $1600 \le Re \le 10{,}700$, $5 \le Pr \le 55$,
$4000 \le Gr \le 2.5\times10^5$, and $1.2 \le \mu_b/\mu_w \le 2.6$

Bell-mouth

$3 \le x/D \le 192$, $3300 \le Re \le 11{,}100$, $13 \le Pr \le 77$,
$6000 \le Gr \le 1.1\times10^5$, and $1.2 \le \mu_b/\mu_w \le 3.1$

Equation (1) is applicable to transition forced and mixed convection in the entrance and fully developed regions and should be used with an appropriate set of constants for each inlet configuration. Figure 4 compares the predicted Nusselt numbers obtained from Eq. (1) for each inlet with measurements. Table 2 summarizes the percent deviations between the experimental data and the predictions of Eq. (1) for the three inlet configurations.

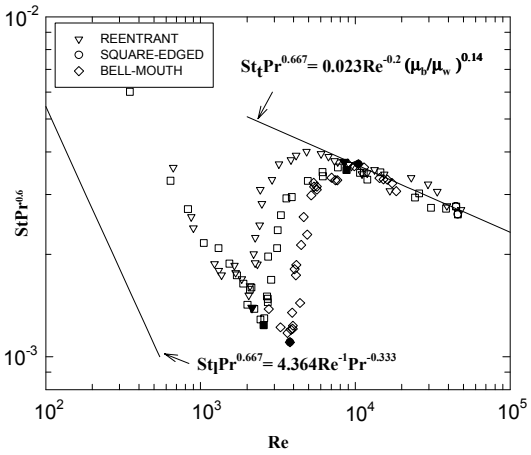

Figure 3 Heat transfer transition region

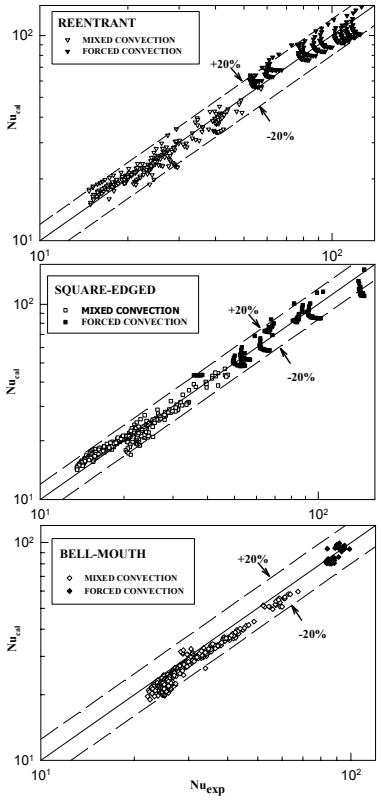

Figure 4 Comparisons between experimental Nusselt numbers and predicted Nusselt numbers using Eq. (1)

Copyright © 2003 by ASME

Table 2. Percent Deviations Between the Experimental Data and Predictions of Eq. (1)

	Reentrant	Square-edged	Bell-mouth
Total data used	441 data points	416 data points	433 data points
Dev. Range	-23 to +25.1%	-23.9 to +24.3%	-22 to +18.5%
> 20% dev.	3% (13pts)	3% (12 pts)	1% (4 pts)
10 to 20% dev.	29% (129pts)	26% (106 pts)	24% (104 pts)
<10% dev.	68% (299 pts)	72% (298 pts)	75% (325 pts)
Avg. abs. dev.	8%	7.2%	8.1%

As seen in Table 2, there is still plenty of room for improving the accuracy of the correlation. Since the accuracy of the heat transfer coefficient will make a direct impact to the size of the heat exchanger, therefore, a correlation with high accuracy using artificial neural network (ANN) is introduced.

The ANN employed in this paper is called a three layer feedforward neural network. Its typical graphical representation is shown in Figure 5.

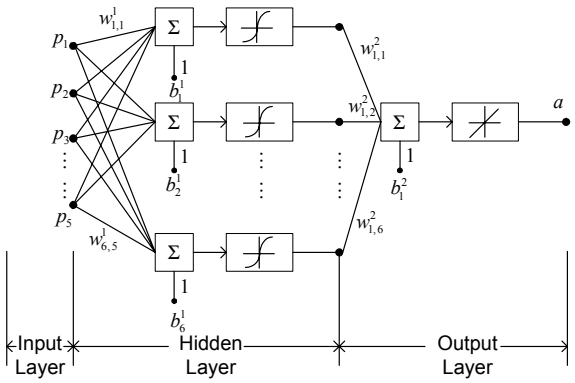

Figure 5 A typical three layer network with six neurons in its hidden layer

In the input layer, the independent variables p_1, p_2,..., p_5 are taken and the s^{th} net input, which is defined as:

$$s^{th} \text{ net input} = \sum_{r=1}^{5} w^1_{s\,r} p_r + b^1_s$$

is fed to the s^{th} neuron of the hidden layer where s=1,2,..,6. Then the neuron converts the net input to a neuron output by utilizing a sigmoid transfer function $f(s) = [1\text{-}\exp(s)]^{-1}$. In the output layer, the s^{th} neuron output is weighted by w^2_{1s}. Finally the unique neuron in the output layer sums all the weighted neuron outputs from the hidden layer and the bias b^2_1 and transforms this sum linearly to produce a number which is the network output. This type of ANN can be used as a high dimensional nonlinear regressor. Precisely, Hornik (1991) has shown that a smooth function defined on any closed and bounded domain of R^n can be smoothly approximated by the type of neural network within a given error bound if we are allowed to increase the number of hidden neurons of the network. Practically, we will fix the number of hidden neurons and identify the other parameters by using a supervised learning algorithm called backpropagation. Basically, backpropagation proposed by Rumelhart et al. (1986) is an algorithm to find the gradient of the square sums of the difference between the network output and the corresponding experimental reading. So the optimum values of parameters w and b can be reached by using a classical gradient based method like steepest descent method. Usually, the gradient method for back-propagation applies the steepest descent algorithm. However, its convergence speed is very slow. More recent algorithms used heuristic techniques such as those by Jacobs (1988) and Vogl et al. (1988), and standard numerical optimization techniques like the work done by Barnard (1992), Batti (1992), and Charalambous (1992) are now available for faster convergence.

In this study, the reentrant data (441 points) is used to determine the type of backpropagation method and the number of neurons used in the hidden layer. The methods to be compared are Steepest Decent Algorithm (SDA), Steepest Descent Algorithm with Variable Learning Rate (SDA-VLR), Conjugate Gradient (CONJUGATE), Quasi-Newton (QN), and the Levenberg-Marquart (LM). The reentrant data was pre-trained/pre-correlated using different methods and different number of neuron combinations. The absolute deviation for the data is used as the method-neuron chosen criteria. The maximum number of iterations was set as 10,000 and all the initial random weights and biases were fixed for each gradient method.

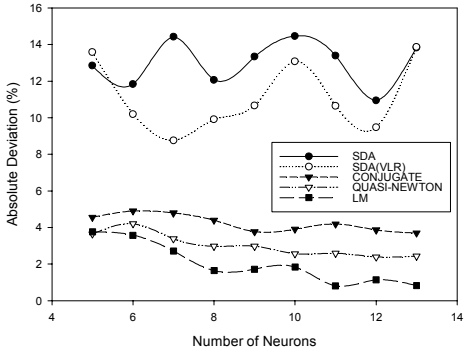

Figure 6 Determination of the method and the number of neurons used

As seen in Fig. 6, when the method is selected as LM and the number of neurons is equaled to 11, the absolute deviation is the smallest amongst all the methods. Therefore, the backpropagation used in this study is the Levenberg-Marquart (LM) method and the number of neurons used in this study is set to 11. Moreover, the learning rate of the LM method is 0.0001. When the epoch reaches 1000, the training stops. After the backpropagation has been completed and the postprocessing of the network output has been performed, the resulted neural network, which is the proposed new correlation, is given in a simple matrix form. The proposed new correlation is as follows.

Copyright © 2003 by ASME

$$Nu = u^3\left\{\left(u^2\right)^T f\left(u^1\Phi + v^1\right) + v^2\right\} + v^3 \qquad (4)$$

where

$$f(s) = [1-\exp(s)]^{-1}$$

$$\Phi = \begin{bmatrix} Re_{normal} \\ Pr_{normal} \\ Gr_{normal} \\ X/D_{normal} \\ \left(\frac{\mu_b}{\mu_w}\right)^{0.14}_{normal} \end{bmatrix} = \begin{bmatrix} 2(Re - Re_{min})/(Re_{max} - Re_{min}) - 1 \\ 2(Pr - Pr_{min})/(Pr_{max} - Pr_{min}) - 1 \\ 2(Gr - Gr_{min})/(Gr_{max} - Gr_{min}) - 1 \\ 2(x/D - x/D_{min})/(x/D_{max} - x/D_{min}) - 1 \\ 2\left(\left(\frac{\mu_b}{\mu_w}\right)^{0.14} - \left(\frac{\mu_b}{\mu_w}\right)^{0.14}_{min}\right)/\left(\left(\frac{\mu_b}{\mu_w}\right)^{0.14}_{max} - \left(\frac{\mu_b}{\mu_w}\right)^{0.14}_{min}\right) - 1 \end{bmatrix}$$

The entries of the vector Φ represent the normalized Reynolds number, Prandtl number, Grashof number, x/D and μ ratio, respectively. In this study, only 80% of the experimental data for each inlet were used to establish the correlation's constant matrices as indicated in Eq. (4). The rest of the data (i.e. 20%) were used for the network testing. The numerical values for the matrices and scalars for different inlet configurations are as follow.

Reentrant Inlet

$$u^1 = \begin{bmatrix} 0.94 & 1.78 & 3.43 & 11.21 & -1.18 \\ 0.42 & -0.01 & 1.39 & -0.03 & 1.62 \\ -7.83 & 14.17 & -5.10 & -0.04 & -0.06 \\ -2.05 & 2.50 & 1.51 & 0.30 & -1.62 \\ -2.90 & -3.60 & 3.07 & -0.10 & -2.73 \\ 2.33 & 1.89 & -0.40 & -0.40 & 1.31 \\ -1.09 & 0.63 & -2.39 & 0.03 & -0.38 \\ -5.89 & -26.99 & -28.11 & 1.84 & -4.98 \\ -0.79 & 0.20 & -2.66 & 0.01 & 0.07 \\ 0.81 & 0.72 & 1.81 & 9.29 & -0.80 \\ -33.66 & 15.59 & 47.16 & 1.00 & -2.20 \end{bmatrix}, \quad u^2 = \begin{bmatrix} 1.20 \\ -9.80 \\ 0.94 \\ 21.41 \\ -2.84 \\ 16.75 \\ -44.09 \\ 0.28 \\ 72.90 \\ -1.80 \\ -0.47 \end{bmatrix}, \quad u^3 = 55.76,$$

$$v^1 = \begin{bmatrix} 13.52 \\ 2.74 \\ -4.54 \\ -0.30 \\ 0.38 \\ 0.85 \\ -3.50 \\ -4.16 \\ -4.43 \\ 13.73 \\ 1.09 \end{bmatrix}, \quad v^2 = 10.01, \quad v^3 = 14.74$$

Square-edged Inlet

$$u^1 = \begin{bmatrix} 0.70 & -1.17 & -26.19 & -6.88 & 4.06 \\ 1.59 & -1.98 & -1.42 & -0.07 & -3.79 \\ -10.53 & 9.63 & 3.71 & 0.43 & -4.41 \\ -0.40 & 1.07 & 21.39 & 6.56 & -3.33 \\ 41.81 & 1.90 & -15.81 & 2.49 & 1.17 \\ -0.37 & -1.18 & 25.86 & -2.23 & 1.11 \\ -16.18 & 12.31 & -8.20 & 0.10 & -4.25 \\ -8.19 & -3.31 & 3.29 & 2.69 & -1.30 \\ 0.87 & -2.03 & -1.04 & -0.19 & -2.49 \\ -1.63 & 0.14 & -0.69 & -0.58 & 4.40 \\ -0.83 & 1.68 & 0.98 & 0.08 & 2.61 \end{bmatrix}, \quad u^2 = \begin{bmatrix} -12.03 \\ 20.36 \\ 3.66 \\ -40.65 \\ 0.37 \\ 0.13 \\ -0.18 \\ -0.19 \\ 14.87 \\ -1.63 \\ 33.98 \end{bmatrix}, \quad u^3 = 66.44,$$

$$v^1 = \begin{bmatrix} -29.45 \\ -4.93 \\ 6.98 \\ 26.55 \\ 12.52 \\ 27.07 \\ -6.65 \\ 0.83 \\ -2.00 \\ 1.30 \\ 2.88 \end{bmatrix}, \quad v^2 = 4.95, \quad v^3 = 13.54$$

Bell-mouth Inlet

$$u^1 = \begin{bmatrix} -0.45 & -7.28 & -3.50 & -0.60 & -6.31 \\ -11.26 & -40.91 & -24.10 & 1.18 & 7.65 \\ -0.66 & -3.13 & -1.12 & 0.94 & 0.51 \\ 2.06 & 6.08 & 3.24 & 3.26 & 1.28 \\ 8.42 & -6.94 & 7.09 & -2.221 & -6.35 \\ 3.29 & -6.77 & 6.76 & -1.12 & -5.01 \\ 1.39 & -1.51 & 1.36 & -0.02 & -0.42 \\ -3.60 & -1.68 & 3.92 & -34.85 & -23.67 \\ 3.88 & 1.86 & -3.04 & -0.53 & -2.41 \\ 1.03 & -1.96 & 0.90 & 0.08 & -0.26 \\ -1.49 & -0.34 & -0.29 & -14.33 & 1.88 \end{bmatrix}, \quad u^2 = \begin{bmatrix} 1.26 \\ 0.10 \\ 1.34 \\ -0.16 \\ 0.61 \\ 0.27 \\ 12.14 \\ -0.02 \\ 0.96 \\ -13.42 \\ 19.24 \end{bmatrix}, \quad u^3 = 46.81,$$

$$v^1 = \begin{bmatrix} -8.43 \\ -19.00 \\ -1.70 \\ 4.99 \\ 0.25 \\ 3.82 \\ 2.25 \\ -24.87 \\ -3.66 \\ 1.58 \\ -19.28 \end{bmatrix}, \quad v^2 = -0.06, \quad v^3 = 22.1$$

Tables 3, 4, and 5 summarize the accuracy of the proposed ANN heat transfer correlations for the three different inlet configurations. Note that for comparison purposes, the tables show the accuracy distribution for 100% of the experimental

Copyright © 2003 by ASME

data (denoted by M), the data that were used to train the network (denoted by M_a -- i.e., 80% of M), and the data that were never used in training but were used for testing (denoted by M_b). Figure 7 compares the predicted Nusselt numbers obtained from the proposed ANN based correlations for each inlet with measurements.

Table 3. Accuracy of the Proposed Reentrant Correlation

Reentrant Inlet, M = 441 pts, M_a = 353 pts, M_b = 88 pts					
	Range of deviation	Absolute deviation	Less than ±5% deviation	Between ±5% and 10% deviation	More than ±10% deviation
M	-11.35% to 7.49%	1.12%	428 data points	12 data points	1 data point
M_a	-8.82% to 7.49%	1.00%	347 data points	6 data points	0 data point
M_b	-11.35% to 6.75%	1.60%	81 data points	6 data points	1 data point

Table 4. Accuracy of the Proposed Square-edged Correlation

Square-edged Inlet, M = 416 pts, M_a = 333 pts, M_b = 83 pts				
	Range of deviation	Absolute deviation	Less than ±5% deviation	Between ±5% and ±10% deviation.
M	-4.88% to 5.24%	1.06%	414 data points	2 data points
M_a	-4.24% to 5.16%	1.03%	332 data points	1 data point
M_b	-4.88% to5.24%	1.16%	82 data points	1 data point

Table 5. Accuracy of the Proposed Bell-mouth Correlation

Bell-mouth Inlet, M = 433 pts, M_a = 347 pts, M_b = 87 pts			
	Range of deviation	Absolute deviation	Less than ±5% deviation
M	-3.45% to 3.60%	0.62%	433 data points
M_a	-2.56% to 2.29%	0.59%	347 data points
M_b	-3.45% to 3.60%	0.74%	87 data points

The proposed ANN correlation is applicable to the developing and fully developed transition regions. As seen in the above tables (Tables 3, 4, and 5) and Fig. 7, for the bell-mouth inlet, all of the experimental data are predicted with less than 5% deviation. For the square-edged inlet, 99.5 percent of the data are predicted with less than 5% deviation. Only 2 data points, one from the training set and the other from the testing set are predicted with a little more than 5% deviation. For the reentrant inlet, practically almost all of the data are predicted with less than 5% deviation (97.1% of the data). Only 12 data points, 6 from the training set and 6 from the testing set are predicted with 5 to 10% deviation, and only one data point is predicted with more than 10% deviation (11.35%). Compared to the accuracy provided by the traditional method, it can be concluded that the ANN correlations outperform the traditional least squares method correlations.

It is worthy to have a discussion to compare the ANN method with the traditional least squares regression method. In Ghajar and Tam (1994), the form of the equation for the least squares regression was determined before the regression.

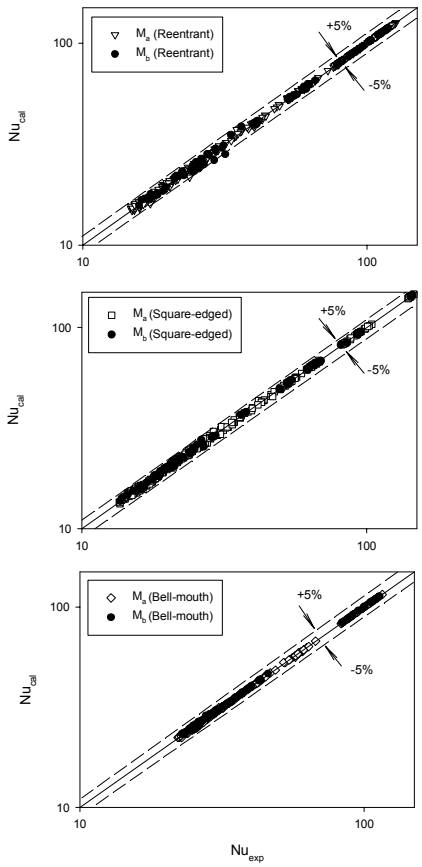

Figure 7 Comparisons between experimental Nusselt numbers and those predicted by the proposed ANN based transition region heat transfer correlation

Determination of the form may not be easy and it is time-consuming. Usually, the form of the correlation is either empirical or semi-empirical and therefore, a lot of unknown factors may influence the accuracy of the correlation. On the other hand, the proposed one hidden layer network, by the theorem of Hornik (1991), has the ability to approximate the unknown nonlinear target correlation by simply choosing an appropriate number of neurons in the hidden layer. By examining the internal structure of the networks, it can be observed that the number of weights and biases will increase or decrease linearly with the input dimension if we add or remove a neuron from the hidden layer, respectively. Due to the linear growth of the parameters, to find a network for better precision, the complexity of the structure of the network would not be influenced significantly by changing the number of hidden neurons. However, for the least squares regression, to improve the precision, it may involve (1) the determination of a better functional form empirically or semi-empirically and/or (2) the addition of extra variables through some difficult experimental processes. For example, in this case, it is necessary

Copyright © 2003 by ASME

to either change the form of Equation (1) or to add one or more independent variables besides Re, Pr, Gr, $(\mu_b/\mu_w)^{0.14}$ and x/D. Both of them are not easy and obvious tasks. Moreover, nontrivial and complicated computation may need to be performed in order to obtain the gradient of the new correlation form for least squares optimization. In this study, we benefited from the back-propagation algorithm, a general way to easily compute the gradient of the kind of networks with various numbers of hidden neurons. Therefore, again according to the linear growth of the parameters and the back-propagation algorithm, the computation complexity is still well under control. Furthermore, unlike the traditional methods, for training a huge amount of experimental data, inexpensive parallel computing using Linux PC cluster can be used in the simulation and the training of ANN to reduce the computational time.

This study provided a new correlation for the heat transfer in the transition region for the three different inlet configurations using an alternative method, which is the artificial neural network (ANN). The heat transfer correlation developed in this study can be used to assist the heat exchanger designer in predicting the heat transfer coefficient along a horizontal straight circular tube with uniform wall heat flux for a specified inlet configuration in the transition region.

REFERENCES

Barnard, E., 1992, Optimization for Training Neural Nets, IEEE Transactions on Neural Networks, Vol.3, No. 2, pp. 232-240.

Batti, R., 1992, First and Second Order Methods for Learning: Between Steepest Descent and Newton's Method, Neural Computation, Vol. 4, No. 2, pp. 141-166.

Charalambous, C., 1992, Conjugate Gradient Algorithm for Efficient Training of Artificial Neural Networks, IEEE Proceedings, Vol. 139, No. 3, pp. 301-310.

Churchill S. W., 1977, Comprehensive Correlating Equations for Heat, Mass and Momentum Transfer in Fully Developed Flow in Smooth Tubes, Ind. Eng. Chem. Fundam., Vol. 16, No. 1, pp.109-116.

Diaz, G., Sen, M., Yang K. T., McClain, R. L., 1999, Simulation of Heat Exchanger Performance by Artificial Neural Networks, HVAC&R Research, Vol. 5, No. 3, pp. 195-208.

Diaz, G. Sen, M., Yang, K. T., McClain, R. L., 2001, Adaptive Neurocontrol of Heat Exchanger, ASME Trans., Vol. 123, pp. 556-562.

Ghajar A. J., Tam L. M., 1994, Heat Transfer Measurements and Correlations in the Transition Region for a Circular Tube with Three Different Inlet Configurations, Experimental Thermal and Fluid Science, Vol. 8, No. 1, pp. 79-90.

Hornik K., 1991, Approximation Capabilities of Multilayer Feedforward Networks, Neural Networks, Vol. 4, No. 2, pp. 251-257.

Jacobs, R.A, 1988, Increased Rates of Convergence Through Learning Rate Adaptation, Neural Networks, Vol. 1, No. 4, pp. 295-308.

Jambunathan, K., Hartle, S. L., Ashforth-Frost, S., and Fontama, V. N., 1996, Evaluating Convective Heat Transfer Coefficients Using Neural Networks, Int. J. Heat Mass Transfer., Vol. 39, No. 11, pp. 2329-2332.

Kakac, S., Shah, R. K., and Bergles, A. E., 1981, Low Reynolds Number Flow Heat Exchanger, Hemisphere, New York.

Kakac, S., Shah, R. K., and Aung, W., 1987, Handbook of Signle-Phase Convective Heat Transfer, Wiley, New York.

Pacheco-Vega, A., Sen, M., Yang, K. T., and McClain, R. L., 2001a, Neural Network Analysis of Fin-Tube Refrigerating Heat Exchanger with Limited Experimental Data, Int. J. of Heat and Mass Transfer, Vol. 44, pp. 763-770.

Pacheco-Vega, A., Diaz, G., Sen, M., Yang, K. T., and McClain, R. L., 2001b, Heat Rate Predictions in Humid Air-Water Heat Exchangers Using Correlations and Neural Networks, ASME Trans., Vol. 123, pp. 348-354.

Rumelhart, D. E., Hinton, G. E., and Williams, R. J., 1986, Learning Internal Representations by Error Propagation, Parallel Distributed Processing: Explorations in the Microstructure of Cognition, (Eds: D. E. Rumelhart, and J. L. McClelland) Vol. 1, MIT Press, Cambridge, Mass., pp. 318-362.

Sen, M., and Yang, K. T., 1999, Applications of Artificial Neural Networks and Genetic Algorithms in Thermal Engineering, CRC Handbook of Thermal Engineering, F. Kreith, ed., Section 4.24, pp. 620-661.

Sieder, E. N., and Tate, G. E., 1936, Heat Transfer and Pressure Drop in Liquids in Tubes, Ind. Eng. Chem., Vol. 28, pp. 1429-1435.

Shah, R. K., and London, A. L., 1978, Laminar Flow Forced Convection in Ducts, a supplement to Advances in Heat Transfer, Academic, New York.

Shah, R. K., and Johnson, R. S., 1981, Correlations for Fully Developed Turbulent Flow Through Circular and Noncircular Channels, Sixth Nat. Heat and Mass Transfer Conf., Indian Inst. Technology, Madras, India, pp. D-75-D95.

Thibault, J., and Grandjean, B. P. A., 1991, A Neural Network Methodology for Heat Transfer Data Analysis, Int. J. Heat Mass Transfer, Vol. 34, No. 8, pp. 2063-2070.

Vogl, T. P., Mangis, J. K., Zigler, A. K., Zink, W. T. and Alkon, D. L., 1988, Accelerating the Convergence of the Backpropagation Method, Biological Cybernetics, Vol. 59, pp. 256-264.

Copyright © 2003 by ASME